

Impact of iron reduction on the metabolism of *Clostridium acetobutylicum*

Cornelia List ¹, Zhaleh Hosseini,²
Karin Lederballe Meibom,¹ Vassily Hatzimanikatis²
and Rizlan Bernier-Latmani ^{1*}

¹Environmental Microbiology Laboratory, Ecole Polytechnique Federale de Lausanne, Lausanne, Switzerland.

²Laboratory of Computational Systems Biotechnology, Ecole Polytechnique Federale de Lausanne, Lausanne, Switzerland.

Summary

Iron is essential for most living organisms. In addition, its biogeochemical cycling influences important processes in the geosphere (e.g., the mobilization or immobilization of trace elements and contaminants). The reduction of Fe(III) to Fe(II) can be catalysed microbially, particularly by metal-respiring bacteria utilizing Fe(III) as a terminal electron acceptor. Furthermore, Gram-positive fermentative iron reducers are known to reduce Fe(III) by using it as a sink for excess reducing equivalents, as a form of enhanced fermentation. Here, we use the Gram-positive fermentative bacterium *Clostridium acetobutylicum* as a model system due to its ability to reduce heavy metals. We investigated the reduction of soluble and solid iron during fermentation. We found that exogenous (resazurin, resorufin, anthraquinone-2,6-disulfonate) as well as endogenous (riboflavin) electron mediators enhance solid iron reduction. In addition, iron reduction buffers the pH, and elicits a shift in the carbon and electron flow to less reduced products relative to fermentation. This study underscores the role fermentative bacteria can play in iron cycling and provides insights into the metabolic profile of coupled fermentation and iron reduction with laboratory experiments and metabolic network modelling.

Introduction

Iron is a transition metal and an element essential for growth and survival of most microorganisms. Not only it

is an important cofactor for the activity of enzymes such as cytochromes and iron–sulfur proteins (Sigel and Sigel, 1998) but can also be used directly as an electron donor or acceptor, depending on its valence state (Weber *et al.*, 2006). Thus, microbial metabolism and metabolic pathways are impacted by iron and its availability. This transition metal is cycled between its Fe(III) and Fe(II) state in nature and these forms are taken up differently by bacteria. The reduced form of iron is easier to acquire from the environment due to its higher solubility compared with Fe(III). Additionally, some bacteria can use Fe(III) as an electron acceptor, producing Fe(II). Aside from metal-respiring bacteria that gain energy directly from electron transport to Fe(III), fermentative iron reducers can use Fe(III) as a sink for excess reducing equivalents as a form of enhanced fermentation (Lovley *et al.*, 2004; Lehours *et al.*, 2010; Dalla Vecchia *et al.*, 2014). However, understanding of the mechanism of iron reduction and the influence of iron on the overall metabolism is limited for fermentative Gram-positive bacteria. These microorganisms are likely to contribute to iron reduction significantly, particularly in environments where Gram-negative bacteria fare poorly, such as metal-contaminated sites or hydrothermal environments (Nepomnyashaya *et al.*, 2010; Burkhardt *et al.*, 2011).

Here, we use the soil bacterium *Clostridium acetobutylicum* as a Gram-positive model organism for acetone–butanol–ethanol (ABE) fermentation and harness its ability to reduce iron and contaminant heavy metals (Jones and Woods, 1986; Gao and Francis, 2008) to study the iron reduction process and its impact on fermentation. The bacterium can utilize a range of monosaccharides and polysaccharides, producing organic acids and solvents (Jones and Woods, 1986). The life cycle of *C. acetobutylicum* is characterized by an initial growth phase in which the organism produces acetate and butyrate as major fermentation products (the acidogenic phase). As the pH value decreases due to the production of these organic acids, the bacterium shifts its metabolism to the production of acetone, butanol and ethanol to overcome the acidification of its environment (the solventogenic phase). In addition, the bacterium also produces H₂ and CO₂ (Jones and Woods, 1986). The coenzyme nicotinamide adenine dinucleotide (phosphate) (NAD(P)) involved in many cellular redox reactions is reduced to NAD(P)H during glycolysis, but must be

Received 16 December, 2018; accepted 22 April, 2019. *For correspondence. E-mail rizlan.bernier-latmani@epfl.ch; Tel. +41 (0)21 693 5001; Fax +41 (0)21 693 6205.

re-oxidized to sustain this glucose oxidation pathway. Thus, NAD(P)H is consumed to generate butyrate during the first phase of the metabolism, but during the solventogenic phase, it is consumed for the production of ethanol and butanol. Furthermore, excess reducing equivalents are transferred onto protons, resulting in H₂ production. If additional electron acceptors such as Fe(III) were provided, the electrons might be delivered to them, instead. The iron reduction process does not contribute significantly to energy conservation, because only a small fraction of excess electrons is directed to iron (Lovley *et al.*, 2004). For that reason, there may be another benefit for fermentative bacteria to reduce heavy metals. A recent study of *Orenia metallireducens* strain Z6, another fermentative bacterium, suggested that iron reduction during fermentation generates energy, but the most significant advantage is that it stabilizes the pH value due to the consumption of protons during the reduction process. Thus, iron reduction indirectly results in higher glucose consumption and a higher growth yield, but less H₂ is produced (Dong *et al.*, 2017). A second study, this time with *Bacillus* sp., showed that the products of fructose fermentation were altered in the presence of Fe(III). They observed decreased lactate production, but increased acetate and CO₂ production in iron-reducing cultures compared to fermentation alone. In addition, the cell density remained constant in stationary phase in iron-reducing cultures, whereas it decreased with fermentation alone (Pollock *et al.*, 2007). Here, we show that *C. acetobutylicum* is able to reduce soluble Fe(III), but solid iron reduction is only significant after the addition of an electron mediator. Iron reduction not only buffers pH but also results in an altered carbon and electron flow. Under iron-reducing conditions, less hydrogen and more butanol are produced during the growth phase compared to fermentation alone. Iron reduction extends the duration of the acidogenic phase resulting in a higher production of organic acid and ATP.

Metabolic modelling confirms the experimental data, as a higher flux variability is obtained if iron is provided suggesting that more alternative reactions are possible for the central metabolic pathways of *C. acetobutylicum* compared with fermentation alone.

Results

Solid iron reduction by *C. acetobutylicum*

Solid iron reduction depends on an exogenous electron shuttle and is impacted by the glucose concentration. Iron reduction assays were performed with a growing culture of *C. acetobutylicum* in mineral salt medium (MSM) containing 0.5% glucose and solid iron as 10 mM hydrous ferric oxide (HFO), with or without an exogenous electron mediator. Electron mediators used in this study were resazurin, resorufin, anthraquinone-2,6-disulfonate (AQDS), riboflavin (RF), flavin mononucleotide (FMN) or flavin adenine dinucleotide (FAD). At 24 h, in medium without electron mediator, *C. acetobutylicum* reduced only 10% of the HFO (1.0 ± 0.4 mM Fe²⁺) (Fig. 1A). However, in medium with electron mediator, HFO reduction increased to 70%–90% (with resazurin: 7.7 ± 1.2 ; with resorufin 7.3 ± 0.2 , with AQDS 9.2 ± 0.5 and with RF 8.6 ± 0.6 mM Fe²⁺) in the same timeline. No increase in HFO reduction occurred with FMN or FAD (data not shown). Based on monitoring the protein concentration, similar growth was observed in the presence of HFO (with or without electron mediator) and in its absence (Fig. 1B).

When resazurin (usually used as a redox indicator, blue dye) was used in the experiments, it was rapidly reduced to resorufin (pink colour) and further to dihydroresorufin (colourless) by *C. acetobutylicum*. The colour changes were detectable visually, but could also be observed by collecting absorbance spectra. In MSM with 100 μ M resazurin, a pronounced resazurin peak was visible at 604 nm, prior

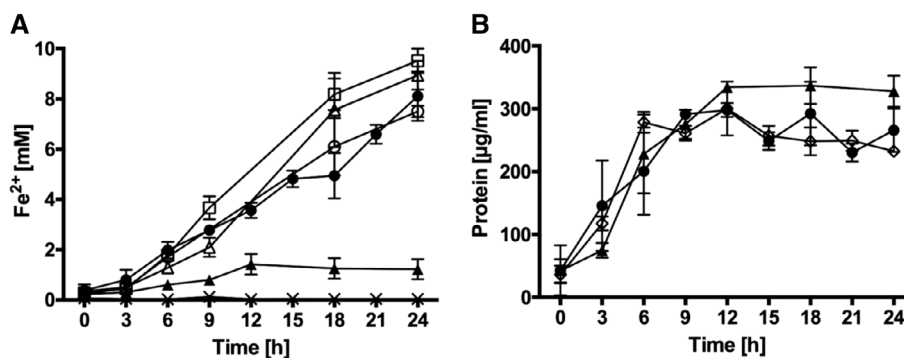


Fig. 1. Solid iron reduction with and without electron mediators.

Clostridium acetobutylicum cultures were grown in MSM with 0.5% glucose, 20 mM MES and 10 mM hydrous ferric oxide (HFO) with resazurin (filled circle), with resorufin (open circle), with AQDS (open square), with RF (open triangle), without electron mediator (filled triangle) and without HFO (open diamond). An abiotic control was used (cross). Fe(II) (A) and protein (B) were measured over time. Error bars indicate results from biological triplicates. HFO reduction was significantly increased in the presence of electron mediators relative to in their absence (multiple *t*-test, Holm-Sidak method, $\alpha = 0.05$).

to inoculation with *C. acetobutylicum* (Fig. S1). To show that the bacterium is able to reduce resazurin, the spectrum was collected again, 5 min after inoculation. The peak decreased and shifted to 570 nm, which represents a reduction of resazurin to resorufin. Finally, the peak disappeared completely after 1 h due to the further reduction of resorufin to dihydroresorufin. Subsequently, the culture was filtered and 10 mM HFO was added to the growth medium. Dihydroresorufin was expected to reduce HFO and, in so doing, should be oxidized to resorufin and the corresponding peak should appear. The appearance of the resorufin peak was confirmed (Fig. S1). Hence, we concluded that the bacterium reduces resorufin to dihydroresorufin, which in turn reduces HFO and is oxidized back to resorufin.

Higher glucose concentrations and varying media were tested in a solid iron reduction assay to determine whether iron reduction could be enhanced in the absence of an exogenous electron mediator. Since more reducing equivalents, which could be directed to iron, are produced with more glucose consumed, higher glucose concentrations were hypothesized to increase the iron reduction rate. Two media (lacking an exogenous electron mediator) were considered: one referred to as clostridium basal medium (CBM) and using a 5% glucose concentration and the other, MSM with 5% glucose (instead of the 0.5% glucose used above). Indeed, with 5% glucose, the bacterium reduced higher amounts of HFO relative to what we observed with 0.5% glucose. In CBM, 26% of 10 mM HFO was reduced at 24 h while 24% was reduced in MSM (Fig. S2).

Solid iron reduction and resazurin shift carbon and electron flow. We probed the hypothesis that iron reduction impacts electron flow and the profile of produced metabolites. The pH value, the concentration of glucose and various metabolites including acetate, butyrate, lactate, acetone, butanol, ethanol, H₂ and CO₂, were measured during fermentation with and without HFO reduction in MSM with resazurin (Fig. 2).

The pH value decreased in the first phase of growth (the first 6 h) with or without HFO. That change correlates with glucose consumption and acid formation. However, the pH in the HFO-reducing cultures did not decrease as much as in the culture without HFO and subsequently increased in the iron-reducing cultures (pH 5–5.6 from 6 to 24 h), while there was no change in pH for the no HFO cultures past 6 h (pH 4.5). Glucose consumption was similar in both conditions and glucose was almost consumed by 6 h. Acetate and butyrate were produced in the first 6 h in both conditions with no obvious difference between the conditions. Lactate was detected at a high concentration (~3 mM) in the absence of HFO and at lower concentration (~1 mM) in its presence. Butanol was produced to a greater extent in the absence of HFO while acetone and ethanol were below the detection limit in all cases (data

not shown). H₂ and CO₂ in the headspace were produced to approximately the same extent for both conditions.

To probe whether resazurin has an influence on fermentation alone, metabolites were measured in the absence and presence of resazurin during fermentation (Fig. S3). In cultures with resazurin, higher amounts of acetate, lactate and butanol were produced compared with fermentation without resazurin, but butyrate and H₂ were lower with resazurin. In cultures during fermentation without resazurin, no lactate was detected.

Soluble iron reduction by C. acetobutylicum

Clostridium acetobutylicum is able to rapidly reduce Fe(III)-citrate. Soluble iron reduction assays were performed with 0.5% glucose and 20 mM Fe(III)-citrate as the iron source. *Clostridium acetobutylicum* reduced 79% of the Fe(III)-citrate (17.31 ± 0.39 mM Fe²⁺) by 24 h (Fig. S4A). In comparison to solid iron reduction, the bacterium rapidly reduced Fe(III) without addition of an extracellular electron mediator. The protein concentration was similar to that in HFO-reducing cultures although the lag phase was longer in the Fe(III)-citrate culture as compared with the no iron culture (Fig. S4B, Fig. 1B). In the abiotic control without bacterial cells, no iron reduction was detectable.

Soluble iron reduction shifts electron and carbon flow. Iron-reducing experiments with varying Fe(III)-citrate concentrations (20, 40 and 50 mM) were performed (in MSM with 4% glucose and 40 mM MES) to decipher the influence of iron concentration on the metabolic profile (Table 1). It is noteworthy that *C. acetobutylicum* did not grow (nor reduced iron) in medium with 100 or 200 mM Fe(III)-citrate (data not shown). In all the cultures with initial concentrations of 20–50 mM Fe(III)-citrate, most of the iron (~90%) was reduced. Just like for HFO, soluble iron reduction starts immediately after inoculation and is still ongoing after glucose is completely consumed. The pH value at 24 h was higher for cultures containing Fe(III)-citrate and increased with increasing Fe(III)-citrate provided. The same was observed with acetate and butyrate (normalized to glucose consumption). In contrast, less butanol was produced per 100 mmol of glucose consumed in cultures with Fe(III) as compared to in the absence of Fe(III)-citrate. H₂ and CO₂ production were highest in the 20 mM Fe(III)-citrate culture, but decreased below fermentation alone concentrations when higher Fe(III)-citrate concentrations were provided.

To assess the effect of iron reduction on the metabolism of *C. acetobutylicum* in more detail, we grew the bacterium in medium with or without addition of Fe(III)-citrate (40 mM), and assessed growth and the metabolic profile at various time points (Fig. 3). The addition of Fe(III)-citrate had no effect on the growth of *C. acetobutylicum*

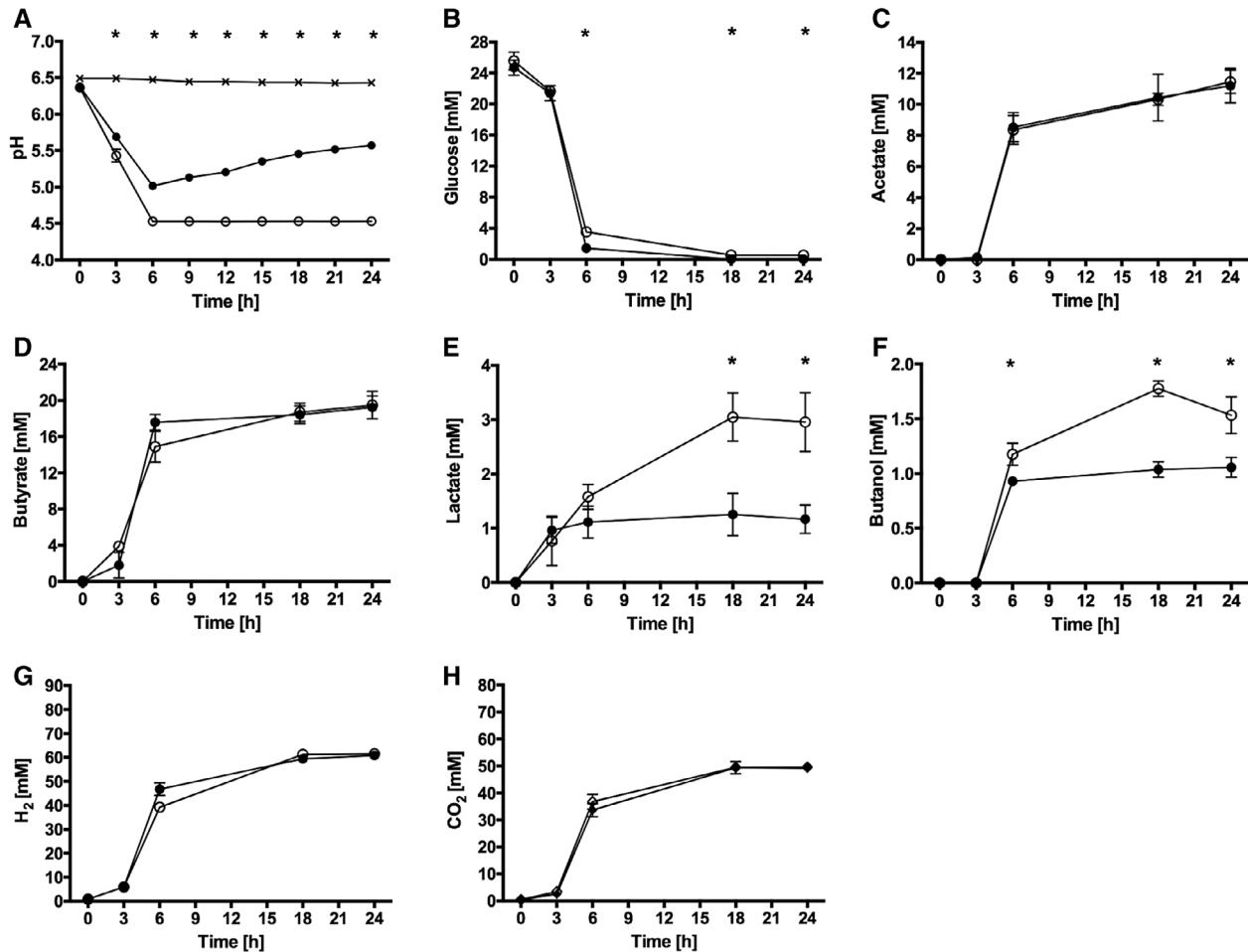


Fig. 2. Metabolites measured during HFO reduction or fermentation alone in MSM with resazurin.

Cultures of *C. acetobutylicum* in MSM with 0.5% glucose, 20 mM MES with resazurin with HFO (filled circle), no HFO (open circle) and an abiotic control without bacterial cells (cross). (A) pH value, (B) glucose, (C) acetate, (D) butyrate, (E) lactate, (F) butanol, (G) H₂ and (H) CO₂ in the headspace. Error bars indicate results from biological triplicates. Asterisks indicate a statistically significant difference between the conditions for each time point (multiple *t*-test, Holm-Sidak method, $\alpha = 0.05$).

(Fig. 3B). The pH value decreases continuously until 18 h in both cultures at which point the pH value is 4.7 ± 0.02 with Fe(III)-citrate and 4.3 ± 0.01 without (Fig. 3C). After 18 h, the pH increases slightly to 4.9 ± 0.04 and 4.5 ± 0.02 respectively.

In both cultures, glucose was consumed to a similar extent until 18 h, but the glucose level remains higher in iron-reducing cultures after this time (Fig. 3D). At 24 h, 36% of the glucose is consumed in cultures with iron, while 50% is consumed in cultures without (Fig. 3D).

Table 1. Metabolites of iron reduction during fermentation with varying ferric iron concentrations.

	Initial Fe ³⁺ in mM	Produced after 24 h							
		mmol/100 mmol consumed glucose							
		Fe ²⁺	Acetate	Butyrate	Butanol	H ₂	CO ₂	OD ₆₀₀	pH
Fermentation	–	–	9.3	21.7	3.4	123.3	153.0	3.9	4.5
Fermentation with Fe(III)-citrate	20	18.6	10.5	31.0	1.5	144.7	180.9	3.5	4.6
	40	41.5	11.1	41.3	0.8	114.3	124.1	2.5	4.9
	50	65.8	19.2	40.3	0.1	45.7	50.7	2.0	5.3

Initial glucose concentration was 216 mM and 40 mM MES was amended.

Note: *Clostridium acetobutylicum* could not grow with medium containing ≥ 100 mM Fe(III)-citrate. A control experiment determined that, starting at 40 mM citrate (no Fe(III)), the citrate concentration is toxic for the organisms, impeding growth.

Acetate production is first detectable at 2 h under both conditions, but between 6 and 12 h, the concentration is up to 1.5-fold greater in cultures without iron compared to cultures with iron (Fig. 3E) (The observed difference between the acetate results in Table 1 and Fig. 3 is attributed to a decrease in growth at 6 h in the iron-reducing case). Butyrate is first detectable at 6 h in cultures without iron and at 8 h in cultures with iron reduction. After 12 h, the butyrate concentration is up to 1.4-fold higher with iron compared to without (Fig. 3F). The concentration of lactate is below the detection limit for both conditions.

The H₂ concentration increases over time after 2 h and is continuously higher in cultures without iron reduction compared to the iron-reducing culture (Fig. 3H). Especially at 8 and 24 h, a clear difference between the two conditions is visible. In cultures without iron, 55.1 ± 0.9 mM H₂ is produced and in cultures with iron reduction 35.9 ± 2.5 mM H₂ is produced at 8 h. At 24 h, the concentration of H₂ is 1.5-fold

higher in cultures without iron reduction (137.9 ± 4.5 mM) compared to cultures with iron reduction (94.2 ± 26.7 mM). The CO₂ concentration in the headspace is similar under both conditions and increases over time (Fig. 3I).

Solvents are detected at the end of the growth phase. Butanol is measurable at 8 h in cultures under both conditions, but higher yields are produced without iron compared to with iron (Fig. 3G). At 24 h, the butanol concentration without iron is 5.9-fold higher than under iron-reducing conditions. *Clostridium acetobutylicum* starts to produce ethanol and acetone at around 18 h under iron-reducing conditions and without iron, but only in small amounts (<0.5 mM) (data not shown).

The concentration of all products normalized to glucose consumed was calculated and the carbon mass balance was verified for both conditions (Table S1). Also, an oxidation–reduction balance was calculated with the amount (mmol) of electrons gained by products relative to glucose (i.e., the reduced products) divided by the

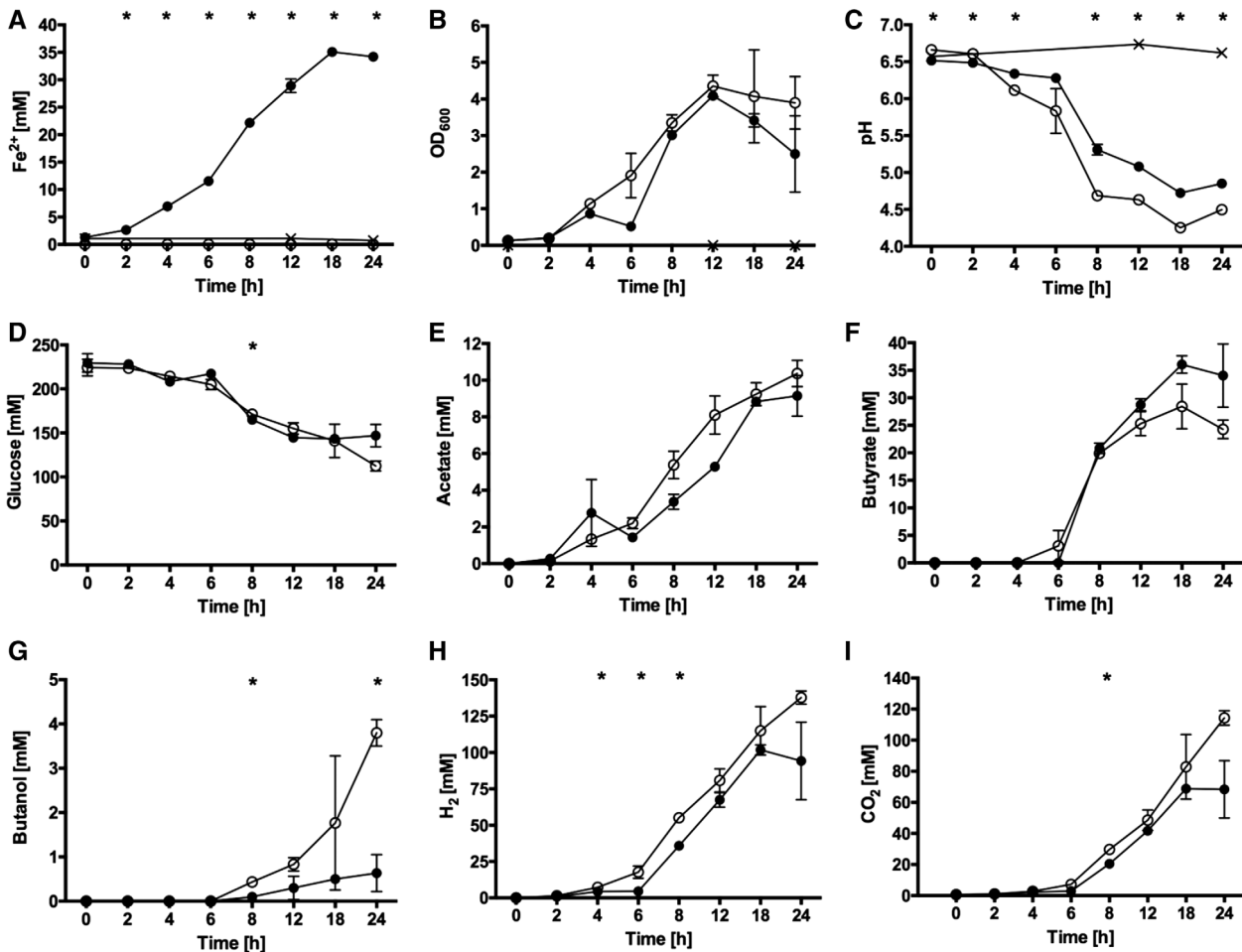


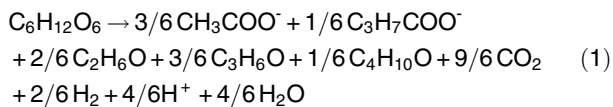
Fig. 3. Metabolic profile of *C. acetobutylicum*.

Cultures with Fe(III)-citrate (filled circle), fermentation alone (open circle) and an abiotic control without bacterial cells (cross). (A) Fe(II), (B) culture density measured as optical density at 600 nm, OD₆₀₀, (C) pH value, (D) glucose, (E) acetate, (F) butyrate, (G) butanol (H) H₂ and (I) CO₂ in the headspace. Error bars indicate results from biological triplicates. Asterisks indicate a statistically significant difference between the conditions for each time point (multiple *t*-test, Holm-Sidak method, $\alpha = 0.05$).

amount (mmol) of electrons lost by glucose to generate oxidized products (see experimental procedures). This value should be 1 if all electrons donated by glucose are accounted for. For fermentation with iron reduction the value is 0.7 and without iron reduction it is 0.9. In addition, ATP production increased during soluble iron reduction with $2.3 \pm 1.1 \mu\text{mol}$ per 100 mmol consumed glucose, compared to fermentation alone with $1.1 \pm 0.5 \mu\text{mol}$ per 100 mmol consumed glucose.

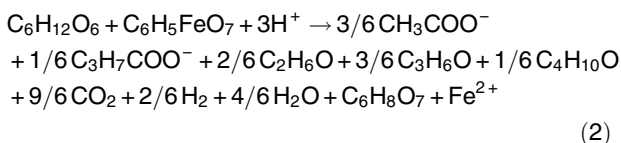
We calculated the Gibbs free energy for fermentation with iron reduction and without. It appears that at 24 h of reaction, fermentation alone is a bit more thermodynamically favourable than fermentation with Fe(III).

For fermentation alone:



$$\Delta G^{\circ} = -245.7 \text{ kJ/reaction}; \Delta G = -565.9.8 \text{ kJ/reaction.}$$

For fermentation with Fe(III)-citrate:



$$\Delta G^{\circ} = -320.0 \text{ kJ/reaction}; \Delta G = -466.8 \text{ kJ/reaction.}$$

Flavins are found in spent growth medium during fermentation by C. acetobutylicum. To determine whether *C. acetobutylicum* secretes an endogenous electron shuttle, iron reduction assays were performed using glass-HFO (where HFO is physically separated from the cells by a glass matrix with a pore size of 50 nm). After 24 h, the organism reduced 6.8% (0.27 mM Fe^{2+}) of glass-associated HFO, which is a similar rate as HFO in suspension suggesting an electron shuttle secreted by the bacterium (and able to diffuse into the pores of glass-HFO) might be involved. In medium with resorufin, it increased to 62% glass-associated HFO reduced ($2.5 \pm 0.2 \text{ mM Fe}^{2+}$) (data not shown).

Probing the culture medium during growth revealed that this bacterium is able to produce flavins during fermentation (Fig. 4). These compounds could potentially act as extracellular electron shuttles. The most common flavins (RF, FMN and FAD) were quantified over time in cultures grown in MSM with 0.5% glucose and with and without resazurin. Cytoplasmic flavins and solution flavins were compared for cultures in the presence and absence of HFO or Fe(III)-citrate as well as in the presence and absence of resazurin (Fig. 4).

FMN and FAD were detected in the cytoplasmic fraction while RF was present at low concentrations (Fig. 4A, C, E).

All flavins were secreted or released to the medium over time (Fig. 4B, D, F) except for FMN, which remains in the cytoplasm in the resazurin-containing HFO-reducing culture and is not detected at high concentrations in the medium for the duration of the experiment (Fig. 4C, D). The extracellular concentration of RF was generally low in most conditions except fermentation with resazurin, where it was measured to be 500 nM (Fig. 4B). The concentration of FAD was higher with fermentation alone with and without resazurin compared to iron-reducing conditions. Interestingly, FAD is detected in the cytoplasmic fraction for all iron-reducing cultures, but the observed decrease in the cytoplasmic concentration was not accompanied by a corresponding increase in the secreted or released fraction.

Metabolic network modelling

Metabolic modelling analysis was performed using the experimental data of the iron reduction experiment with 4% glucose and 40 mM Fe(III)-citrate to constrain the model. The inputs to the metabolic model are the metabolic pathways derived from the genome, and the time-dependent concentrations of substrate and products. The model allows interrogation of several aspects of the metabolism: (i) a comparison of the model predicted flux ranges (in $\text{mmol gDW}^{-1} \text{ h}^{-1}$) for each product to their experimental flux ranges for products, thus providing validation for the model; (ii) a breakdown of the flux ranges according to individual reactions within the metabolic network, allowing the identification of differences in the contribution of specific reactions to the overall flux ranges between conditions (i.e., with and without iron); and (iii) the minimum number of reactions that would support the transformation of substrate to products as observed from the experimental data. The metabolic model of *C. acetobutylicum* did not include any iron reduction reactions. Iron reducing equations either with NAD(P)H or with reduced ferredoxin as a cofactor were added to the model.

The metabolic model shows similar flux ranges compared to experimental data. The flux ranges (minimal and maximal fluxes in $\text{mmol gDW}^{-1} \text{ h}^{-1}$) of the experimental products (acetate, butyrate, butanol and H_2) produced at three time points (4, 6 and 8 h) were compared with theoretical (model-based) metabolites and it was evident that the model largely agrees with the experimental data (Fig. S5). More specifically, the experimental data mainly fell within the predicted flux ranges except for the 8 h time point. At that time point, the model predicted a higher minimal and maximal flux for butyrate and acetate compared to what was obtained experimentally, when Fe(III) was provided. If no Fe(III) is provided, the model predicted minimal and maximal flux ranges that were

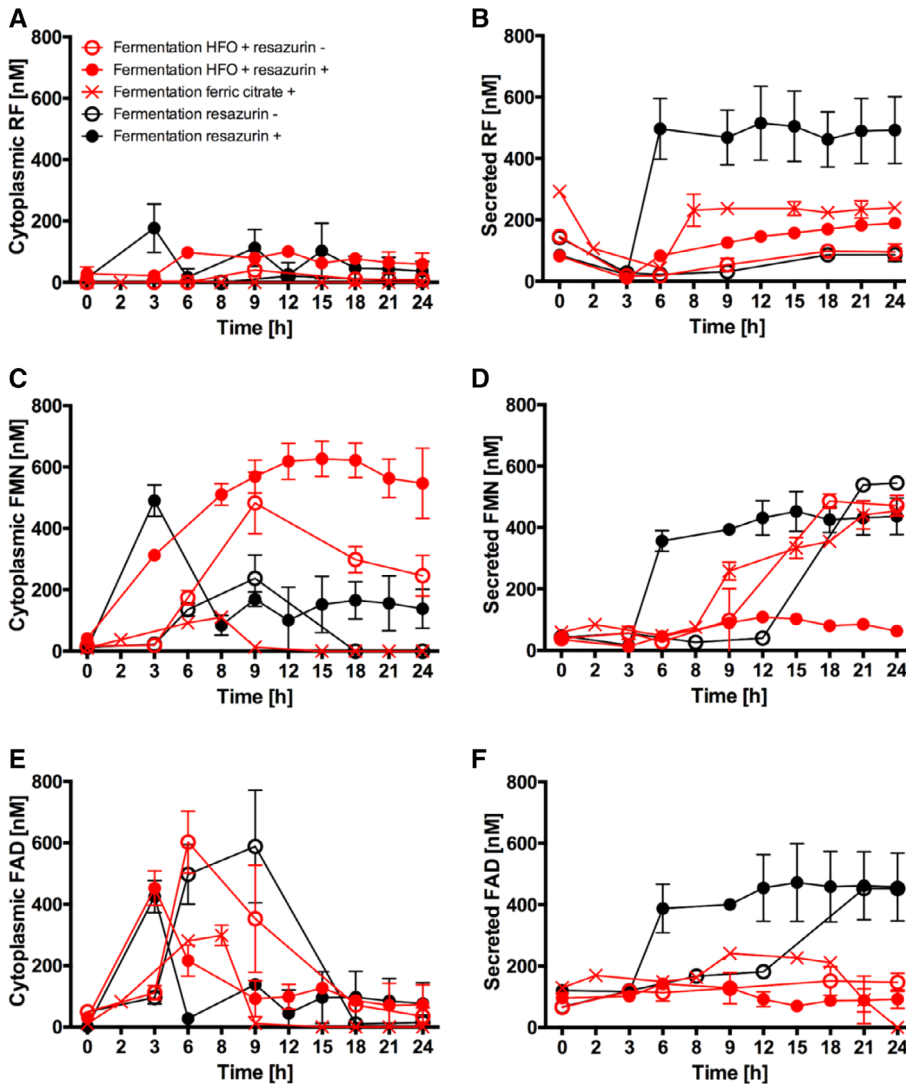


Fig. 4. Flavins during fermentation with and without iron reduction in MSM with and without resazurin. Cytoplasmic (A, C, E) and secreted flavins (B, D, F) of cultures of *C. acetobutylicum* in the presence of solid iron (red circle) or soluble iron (red cross) and in its absence (black) in MSM with 0.5% glucose, 20 mM MES without (empty symbols) and with resazurin (full symbols). The most common flavins were measured, flavin adenine dinucleotide (FAD), flavin mononucleotide (FMN) and riboflavin (RF).

higher for acetate, but lower for H_2 and butyrate compared experimental data.

Higher flux ranges with iron reduction. A flux variability analysis (FVA) was performed to determine whether changes are observed in the metabolic flux ranges with and without iron reduction for central metabolic pathways contained within the model at time point 6 h. If Fe(III)-citrate was provided, there was a distinct shift in the flux ranges (i.e., no overlap in flux ranges). Higher flux ranges were obtained systematically with iron reduction compared to without, for reactions within certain metabolic pathways including glycolysis (glucose 6-phosphate to fructose-6-phosphate and phosphoenolpyruvate to pyruvate) and the citrate acid cycle (oxaloacetate to α -ketoglutarate) (Table S2). Furthermore, in the RF metabolism, the conversion of RF to FMN and FAD was higher with iron reduction. Finally, a large number of anabolic reactions exhibited a larger flux range in the iron case relative to the no

amendment case (Table S2). However, because no pronounced differences in growth were observed in the experimental data, the model was further constrained to minimize the fluxes through anabolic reactions. To visualize both shifts, with and without overlapping flux ranges, the ratio (fermentation with iron reduction/fermentation without iron reduction) of the mean of fluxes is shown in Fig. 5 with NAD(P)H and in Fig. S6 with reduced ferredoxin as the physiological electron donor for iron reduction. In most reactions of the central metabolism, the mean of the flux values is higher with iron reduction (>1), with some exceptions. Using NAD(P)H as the physiological electron donor for iron reduction, a number of reactions exhibited greater flux during fermentation alone: most significantly, a reaction producing ATP (acetyl phosphate + ADP \rightarrow acetate + ATP), one reaction consuming ATP (ribose 5-phosphate + ATP \rightarrow 5-phosphoribosyl 1-pyrophosphate + AMP), the reactions for butanol production, the reaction of D-xylulose 5-phosphate to ribose 5-phosphate and the reaction of 2-deoxy-D-ribose

1-phosphate to glyceraldehyde 3-phosphate (Fig. 5). Using reduced ferredoxin, the result is similar, but higher flux ranges are obtained with fermentation alone for another reaction in the citric acid cycle: succinate to succinyl-CoA consuming ATP and the reduction of NADP with reduced ferredoxin to produce oxidized ferredoxin and NADPH (Fig. S6).

Minimal reaction subnetwork for iron reduction versus fermentation alone. A minimal reaction subnetwork (MRS) provides the minimum number of reactions that are necessary to allow the transformation of a given substrate into given products. There can be more than one MRS for a given substrate/product combination. Reactions that are present in some, but not all of the MRS are termed 'substitutive reactions'. MRSs were computed for fermentation only and iron reduction either with NAD(P)H or with ferredoxin as the physiological electron donor for iron reduction (Fig. 6, Fig. S7). No additional reactions are needed for the reduction of Fe(III) relative to fermentation alone (apart

from the reaction describing the reduction of Fe(III) by NAD(P)H or reduced ferredoxin). If the iron reduction process uses NAD(P)H, the reactions from butyryl-CoA to form butyrate via butyryl phosphate are not necessary for all MRS, whereas they are necessary for fermentation alone or when reduced ferredoxin serves as the physiological electron donor (green, Fig. 6). For fermentation with iron reduction modelled with reduced ferredoxin as the physiological electron donor, more alternative subnetwork reactions can be used with iron reduction using either NAD(P)H or ferredoxin, than without in the fermentation pathway (red, Fig. S7).

In general, the minimal subnetwork using NAD(P)H as a physiological electron donor gives higher flexibility than ferredoxin as an electron donor, due to more alternative pathways.

Excess ATP production calculation. Based on the model, the maximal excess ATP production rate was calculated

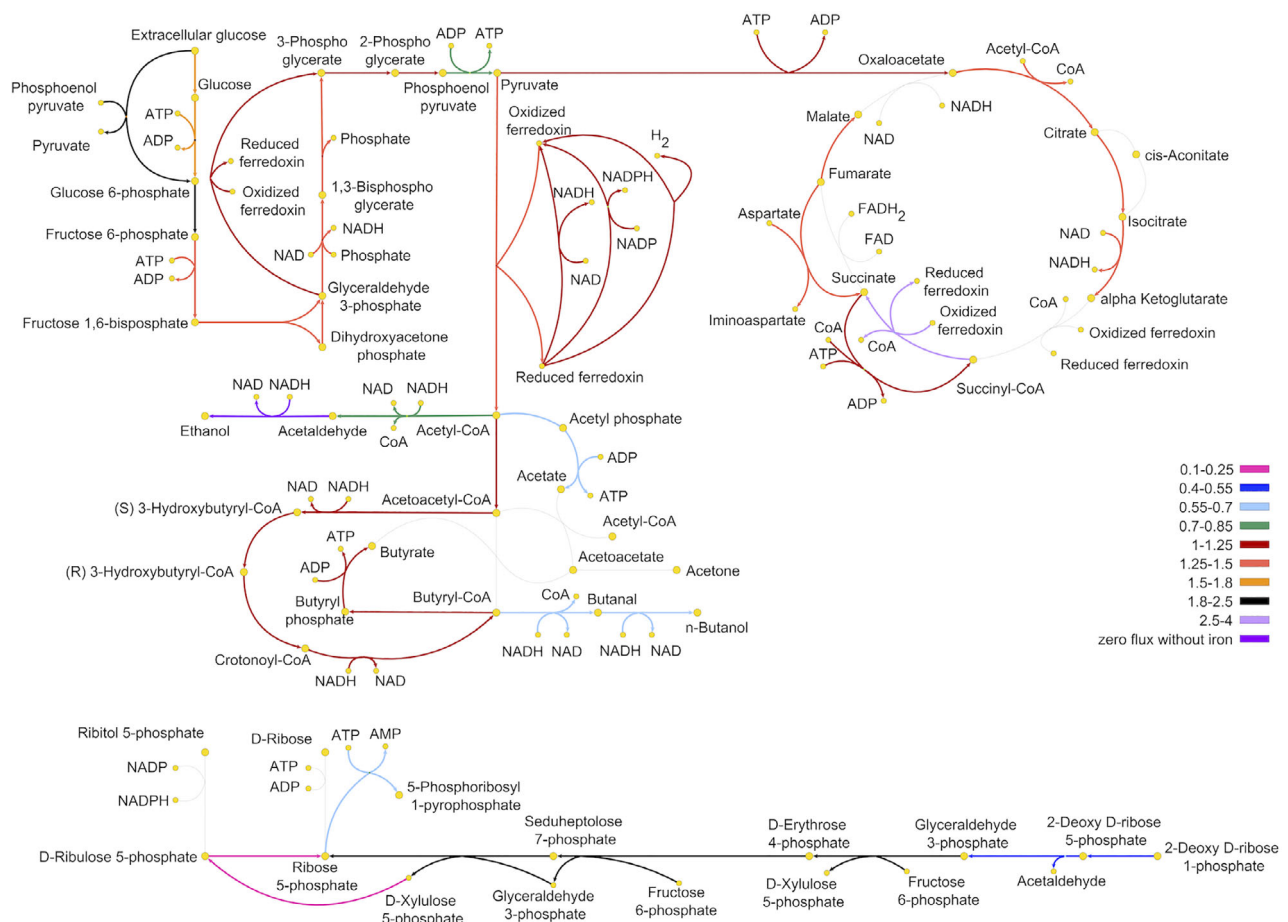


Fig. 5. Flux variability analysis of fermentation with and without iron reduction using NAD(P)H. The mean of flux values (in $\text{mmol gDW}^{-1} \text{h}^{-1}$) from model-based samples was used to calculate the ratio of fermentation with iron reduction divided by fermentation without iron reduction for the reactions of glycolysis, fermentation, citric acid cycle and the pentose phosphate pathway. Grey lines show reactions were no flux was present in the model and gaps in the values within the figure legend indicate that these range was not represented. Flux ranges greater than 1 show reactions with higher flux ranges in fermentation with iron reduction and those less than 1 show those with higher flux ranges in fermentation without iron reduction.

to be $13 \text{ mmol gDW}^{-1} \text{ h}^{-1}$ for fermentation and $15.6 \text{ mmol gDW}^{-1} \text{ h}^{-1}$ during iron reduction by using NAD(P)H as a physiological electron donor. Reduced ferredoxin as a physiological electron donor for iron reduction gives a maximum flux for ATP of $9.6 \text{ mmol gDW}^{-1} \text{ h}^{-1}$.

Discussion

Clostridium acetobutylicum is known for ABE fermentation, but it is also able to reduce metals. Here, we show that the bacterium reduces solid and soluble iron. Whereas soluble iron reduction is very efficient, solid iron is reduced only to a limited extent (Fig. 1, Fig. S4). The iron reduction process is likely different because Fe(III)-citrate can be transported into the cell (Krewulak and Vogel, 2008; Fukushima *et al.*, 2014) where enzymes may reduce it, whereas HFO remains outside the cell requiring either an extracellular

electron transport system to the cell surface or an electron shuttling system for the reduction to occur.

It is well accepted that fermentative iron reducers deliver excess reducing equivalents to Fe(III) as a form of enhanced fermentation (Dalla Vecchia *et al.*, 2014; Dong *et al.*, 2017). Our results show that with a higher substrate (glucose) concentration, the reduction rate of solid iron could be increased likely due to the higher production of excess electrons (Fig. S2). HFO reduction was similar in two media (CBM and MSM) at high glucose concentration, suggesting that the increase in the iron reduction rate (relative to a low glucose system) is a consequence of the higher glucose concentration (Fig. S2). Studies of fermentative solid iron reduction by Gram-positive organisms related to *C. acetobutylicum* showed efficient iron reduction rates, but they grew in the presence of an electron shuttle, natural groundwater or

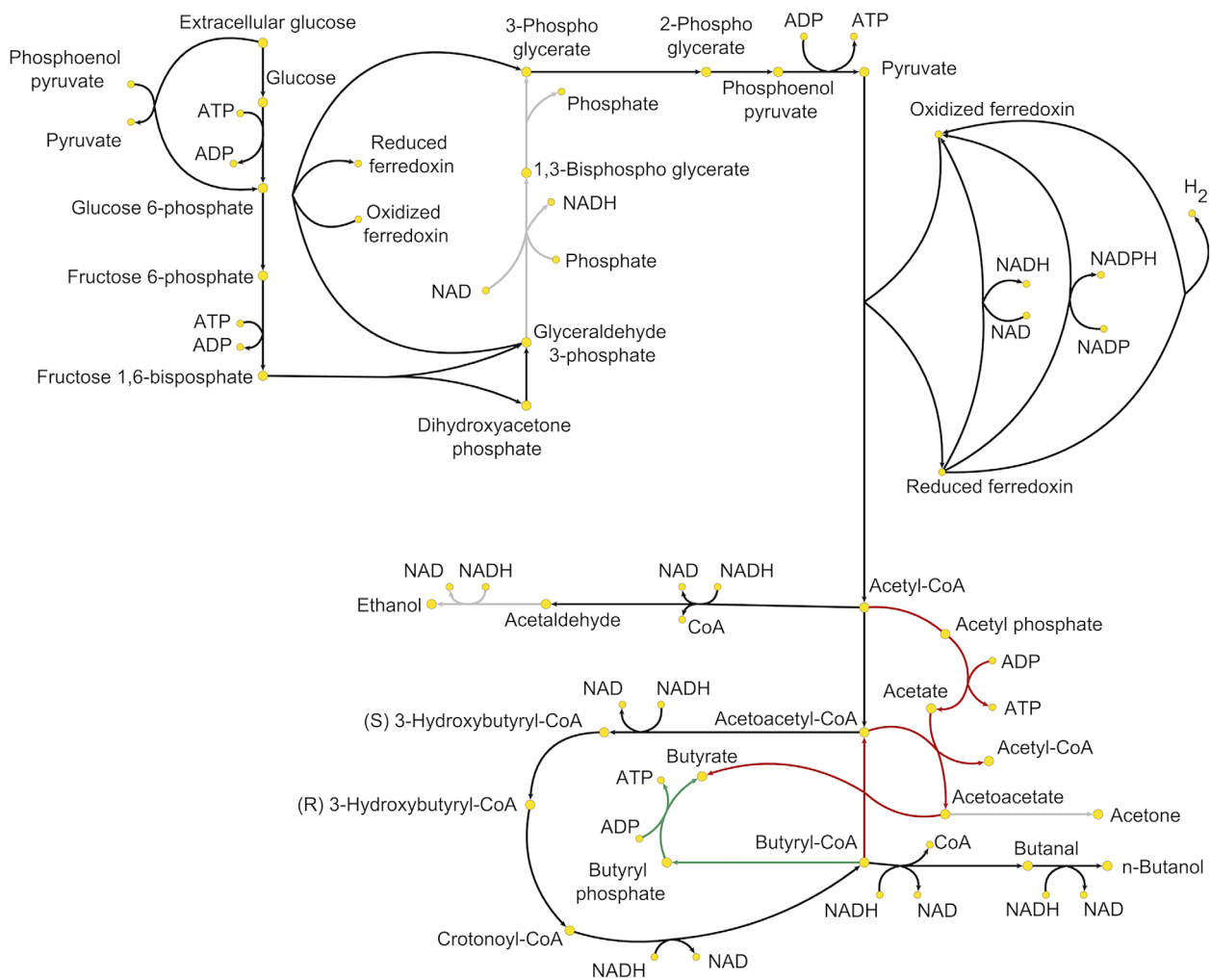


Fig. 6. Minimal reaction subnetwork (MRS) for fermentation with and without iron reduction with NAD(P)H as electron donor.

The minimum reaction set that is necessary to allow the transformation of the substrate into experimental observed products. Black arrows show reactions present in all or some MRS (necessary); green arrows show reactions present in some MRS of fermentation with iron and present in all MRS of fermentation alone; and red arrows show reactions present in some MRS of fermentation with iron, but not present in any MRS of fermentation alone. Grey arrows are reactions not present in the MRS.

sediments (the latter two can contain natural exogenous electron shuttles) (Lehours *et al.*, 2010; Shah *et al.*, 2014; Dong *et al.*, 2016, 2017). Thus, while solid iron reduction by *C. acetobutylicum* is slow in a laboratory setting, soils and sediments are expected to harbour electron shuttles (e.g., humic substances), which may be used by the organisms to transfer electrons to iron oxides. Here, we used artificial electron mediators including resazurin, resorufin, AQDS or an endogenous mediator, RF. Resazurin can be reduced to resorufin with NAD(P)H, FADH or FMNH and further to dihydroresorufin by an unknown mechanism (Rampersad, 2012; Chen *et al.*, 2018). In turn, dihydroresorufin can act as an electron shuttle to reduce HFO, with concurrent oxidation back to resorufin (Fig. S1). Indeed, the rate of solid iron reduction increased dramatically in the presence of resazurin, but also with resorufin, AQDS or RF (Fig. 1), supporting a role for electron shuttles.

During pyruvate fermentation by *Desulfotomaculum reducens*, endogenous flavins were found to reduce solid iron (Dalla Vecchia *et al.*, 2014). The production of flavins under regulation of a putative ferric uptake regulator (Fur) was reported for *C. acetobutylicum* (Vasileva *et al.*, 2012). It was found that RF biosynthesis is increased under iron limitation or in absence of Fur. Flavins are also detected in the fermentation growth medium in this study and may account for the fraction of solid iron reduced by *C. acetobutylicum* in the absence of exogenous shuttles. Flavin secretion is not a known process in Gram-positive bacteria, hence the presence of flavins extracellularly could be due to release by lysis. We probed the extent of cell lysis by measuring viable counts (CFU mL⁻¹) and observed a decrease in CFU mL⁻¹ numbers after 9 h (Fig. S8), raising the possibility that some flavins are released by lysis. However, flavins are measured extracellularly starting at 3 h while CFU mL⁻¹ numbers indicate the exponential growth phase. More importantly, the extracellular flavin concentration is comparable to the intracellular concentration and the intracellular concentration decreases while the extracellular one increases. To account for the extracellular concentration, all the cells would have to lyse, which is clearly not true. Thus, we propose that flavins are secreted through an unknown mechanism because lysis alone cannot account for the extracellular concentration of these compounds. The release of FAD by *C. acetobutylicum* could be due to increased membrane permeability during solventogenesis, which was previously reported (Amador-Noguez *et al.*, 2011). However, in the present study lower amounts of solvents were detected.

In all conditions, FMN is secreted at high concentrations (Fig. 4D). The only exception is in the presence of both HFO and resazurin. In that case, the concentration of secreted FMN is much lower, and the flavin remains in the cytoplasm (Fig. 4D). Additionally, all the three

measured flavins (RF, FMN and FAD) are excreted during fermentation with resazurin. This suggests that FMN (and to a lesser extent RF and FAD) plays a role as a means to deliver electrons to the extracellular milieu. But, why does FMN accumulate intracellularly when both resazurin and HFO are present? We propose that it remains mostly cytoplasmic in the presence of resazurin, because dihydroresorufin reduces HFO efficiently and replaces FMN in its putative role as an electron mediator. Thus, resorufin is re-reduced intracellularly by FMNH, maintaining a specific redox potential. In contrast, in the absence of HFO, dihydroresorufin remains a reduced extracellular molecule, which precludes the oxidation of intracellular flavins by resorufin, and leads to FMN secretion to eliminate excess reducing equivalents.

FAD is produced under all conditions and is secreted in significant amounts during fermentation alone (Fig. 4E, F). Surprisingly, FAD disappears from the cytoplasmic fraction under iron-reducing conditions (i.e., Fe(III)-citrate, HFO with and without resazurin), and is only detected at low concentrations in the medium (HFO case) or disappears from the secreted fraction at later time points (Fe(III)-citrate case) (Fig. 4F). We hypothesize that FAD is hydrolyzed extracellularly to FMN under iron-reducing conditions and covalently bound to a membrane enzyme with a potential role in iron reduction, since the disappearance of FAD is only observed in the iron-reducing cultures. The hydrolysis of FAD to FMN with incorporation into a membrane protein was recently proposed for other Gram-positive bacteria (Buttet *et al.*, 2018). Additionally, a flavin-based extracellular electron transfer mechanism was proposed for Gram-positive bacteria, in which FAD is converted to FMN, which is bound to a predicted extracellular electron transfer lipoprotein (Light *et al.*, 2018). Another possibility is that FAD itself gets incorporated in an insoluble enzyme. Because the intracellular flavin measurement only targets the soluble fraction, no insoluble FMN or FAD (such as that associated with membrane proteins) are detected. The metabolic model predicted an increase in the reaction fluxes towards the conversion of RF to FMN and FAD if Fe(III)-citrate is provided (Table S2).

Interestingly, adding RF as an exogenous electron mediator increased HFO reduction significantly (Fig. 1A) whereas no increase in iron reduction was detected by supplementing the medium with FAD or FMN. One hypothesis could be that, it is a result of flavin transport in *C. acetobutylicum*, which limits the cycling of FMN and FAD if added exogenously. Flavin transporters have not been characterized in *C. acetobutylicum* but the bacterium encodes genes whose corresponding proteins show homology with RF importers in other Firmicutes (Light *et al.*, 2018). As mentioned above, a recent study reported increased RF concentrations in the culture supernatant of

a *fur* mutant or iron-deficient culture suggesting a correlation between RF trafficking and iron availability.

HFO reduction causes a shift in the metabolism of *C. acetobutylicum*. As expected, in cultures without HFO, due to the lack of extracellular terminal electron acceptors, electrons are directed towards butanol, as is typical for solventogenic phase (Fig. 2F). In contrast, in the presence of HFO as an alternative electron acceptor, the electron flow is towards iron and there is a slight increase in the rate production of butyrate and H₂ at intermediate time points (Fig. 2D, G). The production of lactate is also observed to decrease in the presence of HFO (Fig. 2E). Lactate production is not typical for fermentation by *C. acetobutylicum* and is reported under iron-limiting conditions (which is not the case here, data not shown) (Vasileva *et al.*, 2012; Durán-Padilla *et al.*, 2014) and requires further consideration. Investigation of the impact of resazurin alone on the products of glucose fermentation by *C. acetobutylicum* revealed that the electron mediator enhanced acetate, lactate and butanol production substantially (Fig. S3). Conversely, it decreased butyrate and H₂ production (Fig. S3). Thus, when considering the metabolic shift during HFO reduction (Fig. 2), we are actually considering the combined effect of resazurin and HFO on metabolism. Previous studies have documented the shift in metabolism to greater butanol and lactate production in *Clostridium* sp. due to exogenous electron mediators (Peguin *et al.*, 1994; Peguin and Soucaille, 1995; Reimann *et al.*, 1996; Sund *et al.*, 2007; Tashiro *et al.*, 2007; Hönicke *et al.*, 2012; Yarlagadda *et al.*, 2012). In those studies, it was proposed that methyl viologen can replace ferredoxin and thus be preferentially used to generate NADH by the ferredoxin:NAD(P) reductase at the expense of H₂, requiring activation of the lactate dehydrogenase to consume NADH. However, the redox potential of methyl viologen is -0.446 V, but that of resorufin is only -0.051 V (Tratnyek *et al.*, 2001) making it unlikely that it will replace ferredoxin (E_0 -0.430 V). Thus, it is likely that resazurin increases the NADH/NAD ratio through an unknown mechanism, which results in the production of lactate and butanol. Overall, we observed that HFO blunts the impact of resazurin, reducing the production of lactate and butanol and slightly increasing butyrate and H₂ production.

In subsequent experiments, we primarily focused on soluble iron reduction, because of the confounding effect of electron mediators and the highly inefficient reduction of HFO in their absence. *C. acetobutylicum* is able to efficiently deliver 5% of the electrons produced during glycolysis and acetyl-CoA formation to Fe(III)-citrate (provided at a concentration of 40 mM) (Table S1). As a consequence, the carbon and electron flows shift. Compared to fermentation alone, the electron and carbon flows are greater towards butyrate and lower towards butanol. This

may be a consequence of the ability to maintain the pH at higher values due to the consumption of protons in the iron reduction process. In turn, a more stable pH leads to a prolonged acidogenic phase. By directing excess reducing equivalents to organic acid formation and iron reduction, the production of solvents (such as butanol) is decreased. In cultures with 40 and 50 mM Fe(III)-citrate, the H₂ concentration decreased compared to fermentation alone (Table 1). This was not the case with 20 mM Fe(III)-citrate. It appears that, depending on the Fe(III)-citrate concentration, the electron flow towards either butanol and/or H₂ is decreased. This is in accordance with the metabolic network modelling, which includes both the formation of H₂ and butanol in the minimal reaction network for iron reduction (Fig. 6). Similarly, the FVA shows a greater flux towards butyrate in the case that includes iron reduction (Fig. 5).

The highest reduction rate is during the bacterial growth phase, but it is still ongoing after the OD₆₀₀ decreases and glucose consumption has stopped. It was observed in a previous study that electrons are released after electron donor depletion in *D. reducens* during iron reduction (Dalla Vecchia *et al.*, 2014). That study suggested that an intracellular electron storage molecule is involved in the release of electrons to an acceptor. That could be also the case for *C. acetobutylicum* during fermentation under the conditions provided here. No glucose is consumed after 12 h, but iron reduction is still ongoing until 18 h. Potential candidates for electron storage molecules include flavins, which were detected in our study (see above).

Iron reduction buffers the pH as previously described for a fermentative iron-reducing bacterium (Dong *et al.*, 2017). In that study, they noted that due to pH buffering, more substrate was consumed and the growth yield was greater compared to fermentation alone. Similarly, we observe that *C. acetobutylicum* cultures stabilize the pH to greater values under iron-reducing conditions with a pH value up to 0.62 higher than with fermentation alone. However, there is no difference in the consumption of glucose in fermentation with and without iron reduction until 18 h or in the growth yield with *C. acetobutylicum* in our study. Nonetheless, the FVA indicates that anabolism is expected to be greater in the presence of Fe(III)-citrate (Table S2) and ATP production (in excess of maintenance levels) is predicted and measured to be greater with Fe(III)-citrate (Table S1). The absence of experimental evidence for additional growth with iron is attributable to the difference between the two conditions being too small for detection by the tools available. These findings are consistent with greater energy generation, but only through the diversion of electrons from a pathway that does not generate energy (butanol production) to one associated with ATP formation (butyrate production). Interestingly, at 24 h, the glucose concentration

continues to decrease in cultures with fermentation alone, whereas no substrate is further consumed under iron reduction (with 40 mM Fe(III)-citrate) (Fig. 3). Perhaps a second reason for the lack of difference in anabolism between the conditions with and without iron is that elements other than carbon (e.g., nitrogen, sulfur, phosphorus, magnesium and calcium) are limiting glucose consumption (glucose is available in excess).

Considering the fact that during iron reduction, electrons must be directed to Fe(III), one would expect that less NADH is available for the production of butyrate (which requires two NADH molecules to reduce acetoacetate). Hence, it is expected that the acetate/butyrate ratio in iron-reducing cultures would be greater than in cultures with fermentation alone. Interestingly, that is not the case here. In cultures with iron reduction, the acetate/butyrate ratio is 0.27 whereas in cultures with fermentation alone, it is 0.43. However, the increased production of butyrate in iron-reducing cultures mainly occurs between 6 and 18 h. Rather than the redirection of electrons, a more fitting interpretation here is that the shift to solventogenesis is delayed or does not occur at all due to the higher pH. As a result, butyrate is produced at a higher amount, and solvents are almost non-detectable in the iron-reducing cultures. In contrast, in fermentation alone, the organisms switch their metabolism to solventogenesis earlier, directing electrons towards solvent production. The MRS show that (i) iron reduction does not need an additional reaction relative to those for fermentation alone and (ii) iron reduction either via NAD(P)H or reduced ferredoxin provides more alternative pathways for fermentation (Fig. 6, Fig. S7). This flexibility of the organism to have several alternative MRS allows the switch in metabolism due to iron reduction.

Overall, we found that *C. acetobutylicum* uses iron as an alternative electron acceptor causing a reduced decrease in the pH value and allowing acidogenesis to persist for longer. Additionally, there was a shift in the carbon and electron flows as evidenced by the differences in products and the coexistence of more alternative pathways with iron as an electron acceptor in the MRS. Further, *C. acetobutylicum* is able to use resazurin as an exogenous electron mediator, which enhances solid iron reduction and causes an electron and carbon shift distinct from that generated by iron reduction. The experimental data were consistent with the metabolic modelling. In particular, the acidogenic phase persists longer in fermentation with Fe(III), providing the opportunity for the bacterium to gain more energy, which is consistent with the increase in flux for ATP-generating reactions (glycolysis, the citric acid cycle) in the model. Thus, overall, this study provides profound insights into the complex mechanism of this versatile bacterium within soil ecosystems.

Experimental procedures

Cultivation conditions

Clostridium acetobutylicum ATCC 824 was obtained from the Clostridia Research Group at The University of Nottingham. Spores were activated by heat with 80 °C for 10 min and grown on Clostridium Growth Medium agar containing (g L⁻¹): (NH₄)₂SO₄, 2.0; K₂HPO₄, 1.0; KH₂PO₄, 0.5; MgSO₄·7H₂O, 0.1; FeSO₄·7H₂O, 0.015; CaCl₂, 0.01; MnSO₄·H₂O, 0.01; CoCl₂, 0.002; ZnSO₄·7H₂O, 0.002; tryptone, 2.0; yeast extract, 1.0; glucose, 50; agar, 12. After growing 1.5 days on agar plates at 37 °C, several colonies were picked and grown in 2×YTG liquid medium containing (g L⁻¹): tryptone, 16.0; yeast extract, 10.0; sodium chloride, 5.0; glucose, 5 and pH 6 in an anaerobic chamber (COY Laboratory Products, 95.5% N₂, 5% H₂) at 37 °C.

Fermentation and Fe reduction assays

Batch culture experiments were performed in sealed anaerobic serum bottles with butyl rubber stoppers and aluminium crimps at 37 °C. The *C. acetobutylicum* inoculum was grown to mid-exponential phase, and diluted 1:10 in MSM containing (g L⁻¹): NH₄Cl, 0.5; MgSO₄·7H₂O, 0.2; CaCl₂·2H₂O, 2.8; K₂HPO₄, 0.3; peptone, 0.1; yeast extract, 0.1; glycerol, 0.25 mL L⁻¹ and pH 6.8. After the medium was flushed with N₂, the following was added from anaerobic stocks: 10 mg L⁻¹ FeSO₄·7H₂O varying glucose and MES buffer concentrations (see results). For iron reduction assays with an exogenous electron mediator, resazurin, resorufin, AQDS, RF, FMN or FAD was used at a concentration of 4 μM. For the experiment with solid iron in MSM (without resazurin), Clostridium basal medium was used containing (g L⁻¹): MgSO₄·7H₂O, 0.2; MnSO₄·H₂O, 0.00758; FeSO₄·7H₂O, 0.01; *p*-aminobenzoic acid, 0.001; biotin, 0.000002; thiamine hydrochloride, 0.001; casein hydrolysate (enzymatic), 4; K₂HPO₄ and 0.5; KH₂PO₄, 0.5. To probe whether *C. acetobutylicum* reduced resazurin and dihydroresorufin reduces HFO by measuring the absorbance spectra, concentrations of 100 μM of resazurin and of 10 mM HFO were used.

For Fe reduction assays, the medium was amended with HFO, HFO embedded in glass particles (glass-HFO) (Dalla Vecchia *et al.*, 2014) or Fe(III)-citrate. HFO was prepared under sterile conditions with Fe(III)-chloride by slowly increasing the pH to 6.5. The suspension was centrifuged at 8000 rcf for 10 min at room temperature, washed with Milli-Q water three times and resuspended in Milli-Q water. The Fe(III)-citrate stock was prepared as follows (g L⁻¹): Fe(III)-citrate (Sigma-Aldrich, BioReagent, suitable for cell culture), 24.49; NaOH, 6.8; after dissolving by heat and cooling, the stock solution was

flushed with N₂ and stored anaerobically at 4 °C. Samples were collected over time under anaerobic conditions. For all conditions, triplicates cultures were prepared and an abiotic control without bacterial cells included, except for fermentation with 0.5% glucose (20 mM MES without resazurin), solid iron reduction in CBM and MSM with 5% glucose and in fermentation with 50 mM Fe(III)-citrate. For gas sampling, the experiment was performed with extra culture bottles for each sampling point and the culture bottle was sacrificed to ensure a representative gaseous phase composition.

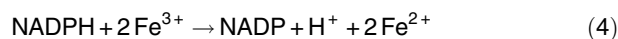
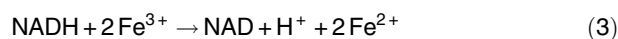
Analytical methods

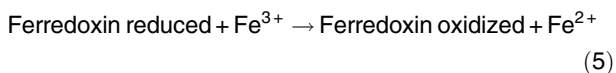
Growth was estimated by measuring the culture density (measured as optical density at 600 nm, OD₆₀₀) or determined via protein measurements (Pierce BCA Protein Assay Kit - Thermo Fisher Scientific) after cell lysis (lysis buffer: 0.1% triton X-100, 0.1% SDS, 10 mM EDTA and 1 mM TrisHCl) at 95 °C for 10 min. The samples were measured in 96-well plates in a BioTek Synergy™ Mx microplate reader. The absorbance spectra of resazurin and resorufin were measured in anaerobic cuvettes with a spectrophotometer (UV-2501PC, UV-VIS recording spectrophotometer; Shimadzu, Reinach, Switzerland). In addition, CFU mL⁻¹ was determined by plating a dilution of the culture sample at different time points on CGM agar plates and counting the resulting CFU after 24 h. The pH was measured directly after sampling with a pH meter (Thermo Scientific™ Orion™ 3-Star Benchtop). Headspace samples were stored in vacuumed serum bottles sealed with butyl rubber stoppers and aluminium crimps prior to injection in a GC-450 (Varian, Middelburg, The Netherlands) using a molecular sieve column (CP81071: 1.5 m × 1/8" ultimetalsieve 13 9 80–100 mesh) and a thermal conductivity detector. Filtered samples for Fe analysis were acidified immediately and stored at 4 °C before analysis via the ferrozine assay (Dalla Vecchia *et al.*, 2014). The samples were diluted in a ferrozine solution (1 g L⁻¹ ferrozine in 100 mM Hepes) and Fe quantified by measuring the absorbance at 562 nm (Bio Spectrometer Eppendorf). Fermentation metabolites were analysed from the supernatant (after filtration of a culture aliquot with a 0.22 µm filter) of the assay culture. These samples were stored in sealed tubes at -20 °C prior to analysis. Glucose, pyruvate, organic acids and solvents were quantified using high-performance liquid chromatography (HPLC) and a refractive index detector (1260 Infinity II). Samples were eluted through a PL Hi-Plex H guard column 50 × 7.7 mm and a Hi-Plex H column (7.7 × 300 mm, 8 µm, p/n PL1170-6830, Agilent Technologies) with 0.0085 M H₂SO₄ as an isocratic eluent. The ethanol concentration in the experiment with solid iron reduction and

resorufin was very noisy due to the use of ethanol to disinfect the surface of the stopper before sampling (data not shown). The most common flavins, RF, FMN and FAD were quantified with HPLC (with a C18 polymeric reversed-phase, non-encapped, 300 Å pore, 201TP54 4.6 × 250 mm, 5 µm, Vydac) with a fluorescent light detector (1260 FLD Spectra, Agilent Technologies) set at λ_{ex} = 445 nm and λ_{em} = 530 nm. A protocol slightly modified from Capo-chichi *et al.* (2000) was used with an isocratic eluent (15% acetonitrile in 10 mM KH₂PO₄ and 15 mM (CH₃COO)₂Mg, pH 3.4) and a flow rate of 0.5 mL min⁻¹ for 13 min. The total flavins were measured by lysing 1 mL of the culture, centrifugation of the cell debris and measuring the supernatant. In addition, the supernatant of the culture (without cell lysis) was also sampled and measured directly. Cytoplasmic flavins were then calculated by subtracting the concentrations of flavins in the supernatant sample. The total inorganic (TIC) and organic carbon (TOC) were determined via a total organic carbon analyser (TOC-V_{CPH}, Shimadzu). The sample for TIC was amended with NaOH to a pH value >12 to keep the carbonate in solution and then centrifuged. The supernatant as well as the pellet were collected and stored at 4 °C prior analysis. The supernatant as well as the pellet were analysed separately for TIC and TOC. The same was done for TOC samples, but instead of NaOH amendment, the samples were acidified. Samples for determining the ATP concentration were immediately frozen at -20 °C. The samples were measured using the ATPlite luminescence assay system (Perkin-Elmer) in 96-well plates (white) and a BioTek Synergy Mx microplate reader. In all graphs, the average with standard deviation is shown. For statistical analysis a multiple *t*-test (Holm-Sidak method, α = 0.05) was used. The oxidation–reduction balance was calculated by dividing the oxidation state of the reduced products by the oxidized products relative to glucose as follows (in mmol): mmol acetate*0 + mmol butyrate*4 + mmol ethanol*4 + mmol acetone*4 + mmol butanol*8 + mmol H₂*2 + mmol Fe²⁺*1 divided by mmol pyruvate*2 + mmol CO₂*4 + mmol TIC*4. In addition, ATP was measured.

Metabolic network modelling

Metabolic analysis was performed with the experimental data of the Fe(III)-citrate reduction experiment. *iCac802* was used as the genome-scale model (Dash *et al.*, 2014). The original model contains 1457 reactions and 1247 metabolites. To be able to model iron reduction, the three following reactions were added to the model one at a time and results were compared with the condition with no iron:





Uptake flux rates for glucose and iron and secretion flux rates for acetate, butyrate, butanol, H₂ and CO₂ were also calculated after polynomial fitting to experimental concentration data. These flux rates were used to constrain the corresponding uptake and secretion rates in the model and to compare the results of model simulation with experimental measurements. Metabolic network models are usually studied using flux balance analysis (FBA) (Orth *et al.*, 2010). In FBA, an objective function in the model is optimized subject to stoichiometric and capacity constraints. Here, thermodynamic-based flux balance analysis (TFA) was used for studying iron reduction in *iCac802*. In TFA, metabolite concentrations and Gibbs free energy of reactions are also taken into account (Henry *et al.*, 2007). To check the consistency between model and experimental data, all above-mentioned constraints except the growth rates for metabolite secretions and uptakes were put as lower and upper bounds of the corresponding fluxes in the metabolic network. The experimental standard deviations were used to calculate the lower and upper bounds put into the model. Then, the model was optimized by maximizing the biomass production and it was compared with the experimental data of growth rates. After maximizing biomass production, the lower bound for biomass reaction was set to 90% of its maximum and then FVA was performed to identify reactions that shifted fluxes when the appropriate iron reduction reaction is added to the model. Sampling of the solution space was done to see the change in the mean value of the reactions involved in glycolysis, citric acid cycle, fermentation and pentose phosphate pathway. For doing so, the minimum amount of acetate needed to be produced from central fluxes to fulfil experimental constraints was calculated and was set as a new constrain to the model. The reactions from acetoacetyl-CoA to acetoacetate and butyryl-CoA to butyrate were forced to only carry fluxes in the forward direction. After sampling 5000 points, the mean value of the reactions in the no iron condition was divided by the mean value of the reactions with iron-reducing conditions. Moreover, to compare the experimental and theoretical flux ranges for acetate, butyrate, butanol and H₂ the bounds on these fluxes were relaxed and the maximum and minimum possible fluxes were calculated for each. To calculate ATP production, the predetermined bounds on ATP maintenance reaction were relaxed and maximum flux for this reaction was calculated for each of the iron-reducing reactions, while maintaining the experimental constrains. The results were compared with the no Fe(III) case. Finally, all alternative MRS s were constructed by setting all experimental data as constraints. Metabolic graphs were drawn using yEd graph editor.

Acknowledgements

We are grateful for assistance provided by the Clostridia Research Group at The University of Nottingham. We would like to acknowledge D. Grandjean for his assistance with HPLC measurements and Dr. J. Maillard for helpful discussions. The work was funded by the Swiss National Science Foundation Grants 310030_156957 and 310030_176146.

Conflict of Interest

The authors declare that they have no conflict of interest.

References

- Amador-Noguez, D., Brasg, I.A., Feng, X.-J., Roquet, N., and Rabinowitz, J.D. (2011) Metabolome remodeling during the acidogenic-solventogenic transition in *Clostridium acetobutylicum*. *Appl Environ Microbiol* **77**: 7984–7997.
- Burkhardt, E.-M., Bischoff, S., Akob, D.M., Büchel, G., and Küsel, K. (2011) Heavy metal tolerance of Fe(III)-reducing microbial communities in contaminated creek bank soils. *Appl Environ Microbiol* **77**: 3132–3136.
- Buttet, G.F., Willemin, M.S., Hamelin, R., Rupakula, A., and Maillard, J. (2018) The membrane-bound C subunit of reductive dehalogenases: topology analysis and reconstitution of the FMN-binding domain of PceC. *Front Microbiol* **9**: 755.
- Capo-chichi, C.D., Guéant, J.L., Feillet, F., Namour, F., and Vidailhet, M. (2000) Analysis of riboflavin and riboflavin cofactor levels in plasma by high-performance liquid chromatography. *J Chromatogr B Biomed Sci Appl* **739**: 219–224.
- Chen, J.L., Steele, T.W.J., and Stuckey, D.C. (2018) Metabolic reduction of resazurin; location within the cell for cytotoxicity assays. *Biotechnol Bioeng* **115**: 351–358.
- Dalla Vecchia, E., Suvorova, E.I., Maillard, J., and Bernier-Latmani, R. (2014) Fe(III) reduction during pyruvate fermentation by *Desulfotomaculum reducens* strain MI-1. *Geobiology* **12**: 48–61.
- Dash, S., Mueller, T.J., Venkataramanan, K.P., Papoutsakis, E. T., and Maranas, C.D. (2014) Capturing the response of *Clostridium acetobutylicum* to chemical stressors using a regulated genome-scale metabolic model. *Biotechnol Biofuels* **7**: 144.
- Dong, Y., Sanford, R.A., Boyanov, M.I., Kemner, K.M., Flynn, T.M., O'Loughlin, E.J., *et al.* (2016) *Orenia metallireducens* sp. nov. strain Z6, a novel metal-reducing member of the phylum firmicutes from the deep subsurface. *Appl Environ Microbiol* **82**: 6440–6453.
- Dong, Y., Sanford, R.A., Chang, Y., McInerney, M.J., and Fouke, B.W. (2017) Hematite reduction buffers acid generation and enhances nutrient uptake by a fermentative iron reducing bacterium, *Orenia metallireducens* strain Z6. *Environ Sci Technol* **51**: 232–242.
- Durán-Padilla, V.R., Davila-Vazquez, G., Chávez-Vela, N.A., Tinoco-Valencia, J.R., and Jáuregui-Rincón, J. (2014) Iron effect on the fermentative metabolism of *Clostridium acetobutylicum* ATCC 824 using cheese whey as substrate. *Biofuel Res J* **1**: 129–133.

- Fukushima, T., Allred, B.E., and Raymond, K.N. (2014) Direct evidence of iron uptake by the Gram-positive siderophore-shuttle mechanism without iron reduction. *ACS Chem Biol* **9**: 2092–2100.
- Gao, W., and Francis, A.J. (2008) Reduction of uranium(VI) to uranium(IV) by Clostridia. *Appl Environ Microbiol* **74**: 4580–4584.
- Henry, C.S., Broadbelt, L.J., and Hatzimanikatis, V. (2007) Thermodynamics-based metabolic flux analysis. *Biophys J* **92**: 1792–1805.
- Hönicke, D., Janssen, H., Grimmer, C., Ehrenreich, A., and Lütke-Eversloh, T. (2012) Global transcriptional changes of *Clostridium acetobutylicum* cultures with increased butanol:acetone ratios. *N Biotechnol* **29**: 485–493.
- Jones, D.T., and Woods, D.R. (1986) Acetone-butanol fermentation revisited. *Microbiol Rev* **50**: 484–524.
- Krewulak, K.D., and Vogel, H.J. (2008) Structural biology of bacterial iron uptake. *Biochim Biophys Acta BBA - Bioembr* **1778**: 1781–1804.
- Lehours, A.-C., Rabiet, M., Morel-Desrosiers, N., Morel, J.-P., Jouve, L., Arbeille, B., et al. (2010) Ferric iron reduction by fermentative strain BS2 isolated from an iron-rich anoxic environment (Lake Pavin, France). *Geomicrobiol J* **27**: 714–722.
- Light, S.H., Su, L., Rivera-Lugo, R., Comejo, J.A., Louie, A., lavarone, A.T., et al. (2018) A flavin-based extracellular electron transfer mechanism in diverse Gram-positive bacteria. *Nature* **562**: 140–144.
- Lovley, D.R., Holmes, D.E., and Nevin, K.P. (2004) Dissimilatory Fe(III) and Mn(IV) reduction. *Adv Microb Physiol* **49**: 219–286.
- Nepomnyashaya, Y.N., Slobodkina, G.B., Kolganova, T.V., Bonch-Osmolovskaya, E.A., Netrusov, A.I., and Slobodkin, A.I. (2010) Phylogenetic composition of enrichment cultures of thermophilic prokaryotes reducing poorly crystalline Fe(III) oxide with and without direct contact between the cells and mineral. *Microbiology* **79**: 663–671.
- Orth, J.D., Thiele, I., and Palsson, B.Ø. (2010) What is flux balance analysis? *Nat Biotechnol* **28**: 245–248.
- Peguín, S., and Soucaille, P. (1995) Modulation of carbon and electron flow in *Clostridium acetobutylicum* by iron limitation and methyl viologen addition. *Appl Environ Microbiol* **61**: 403–405.
- Peguín, S., Goma, G., Delorme, P., and Soucaille, P. (1994) Metabolic flexibility of *Clostridium acetobutylicum* in response to methyl viologen addition. *Appl Microbiol Biotechnol* **42**: 611–616.
- Pollock, J., Weber, K.A., Lack, J., Achenbach, L.A., Mormile, M.R., and Coates, J.D. (2007) Alkaline iron(III) reduction by a novel alkaliphilic, halotolerant, *Bacillus* sp. isolated from salt flat sediments of Soap Lake. *Appl Microbiol Biotechnol* **77**: 927–934.
- Rampersad, S.N. (2012) Multiple applications of Alamar blue as an indicator of metabolic function and cellular health in cell viability bioassays. *Sensors* **12**: 12347–12360.
- Reimann, A., Biebl, H., and Deckwer, W.-D. (1996) Influence of iron, phosphate and methyl viologen on glycerol fermentation of *Clostridium butyricum*. *Appl Microbiol Biotechnol* **45**: 47–50.
- Shah, M., Lin, C.-C., Kukkadapu, R., Engelhard, M.H., Zhao, X., Wang, Y., et al. (2014) Syntrophic effects in a subsurface clostridial consortium on Fe(III)-(Oxyhydr)oxide reduction and secondary mineralization. *Geomicrobiol J* **31**: 101–115.
- Sigel, A., and Sigel, H. (1998) Metal ions in biological systems, volume 35: iron transport and storage microorganisms, plants, and animals. *Met Based Drugs* **5**: 262–262.
- Sund, C.J., McMasters, S., Crittenden, S.R., Harrell, L.E., and Sumner, J.J. (2007) Effect of electron mediators on current generation and fermentation in a microbial fuel cell. *Appl Microbiol Biotechnol* **76**: 561–568.
- Tashiro, Y., Shinto, H., Hayashi, M., Baba, S.-I., Kobayashi, G., and Sonomoto, K. (2007) Novel high-efficient butanol production from butyrate by non-growing *Clostridium saccharoperbutylacetonicum* N1-4 (ATCC 13564) with methyl viologen. *J Biosci Bioeng* **104**: 238–240.
- Tratnyek, P.G., Reilkoff, T.E., Lemon, A.W., Scherer, M.M., Balko, B.A., Feik, L.M., and Henegar, B.D. (2001) Visualizing redox chemistry: probing environmental oxidation-reduction reactions with indicator dyes. *Chem Educ* **6**: 172–179.
- Vasileva, D., Janssen, H., Hönicke, D., Ehrenreich, A., and Bahl, H. (2012) Effect of iron limitation and fur gene inactivation on the transcriptional profile of the strict anaerobe *Clostridium acetobutylicum*. *Microbiology* **158**: 1918–1929.
- Weber, K.A., Achenbach, L.A., and Coates, J.D. (2006) Microorganisms pumping iron: anaerobic microbial iron oxidation and reduction. *Nat Rev Microbiol* **4**: 752–764.
- Yarlagadda, V.N., Gupta, A., Dodge, C.J., and Francis, A.J. (2012) Effect of exogenous electron shuttles on growth and fermentative metabolism in *Clostridium* sp. BC1. *Bio-resour Technol* **108**: 295–299.

Supporting Information

Additional Supporting Information may be found in the online version of this article at the publisher's web-site:

Fig. S1. Absorbance spectra of MSM with resazurin before and after inoculation. The absorbance spectrum of MSM with resazurin was measured before inoculation with *C. acetobutylicum* (dotted line), 5 min (dashed line) and 1 h (green) after inoculation and after filtration of the culture and addition of HFO to the supernatant (solid line). The absorbance peak of resazurin is at 604 nm and of resorufin at 570 nm. Dihydroresorufin does not exhibit an absorbance spectrum at this range of wavelengths.

Fig. S2. Solid iron reduction in MSM or CBM with 5% glucose. *C. acetobutylicum* cultures were grown in MSM (open cycle) or CBM (filled cycle) with 5% glucose, 20 mM MES and 10 mM hydrous ferric oxide (HFO) and ferrous iron was measured over time.

Fig. S3. Metabolites measured during fermentation with or without resazurin. Cultures of *C. acetobutylicum* in MSM with 0.5% glucose, 20 mM MES with resazurin (filled squares) and without resazurin (open squares). (A) protein, (B) glucose, (C) acetate, (D) butyrate, (E) lactate, (F) butanol (G) H₂ and (H) CO₂. Error bars indicate results from biological triplicates.

Fig. S4. Soluble iron reduction. The cultures were grown in MSM with 0.5% glucose, 20 mM MES with 20 mM Fe(III)-citrate (filled circles) or without Fe(III)-citrate (open circles). An abiotic control was used (cross). (A) ferrous iron and (B) protein.

Fig. S5. Flux ranges of experimental metabolites compared with theoretical (model based) metabolites of fermentation with and without Fe(III)-citrate. The minimal flux and the maximal flux of acetate, butyrate, butanol and H₂ were compared of experimental data (blue) and model predicted data (red) by using NAD(P)H as physiological electron donor.

Fig. S6. Flux variability analysis of fermentation with and without iron reduction using reduced ferredoxin. The mean of flux values (in mmol/gDW/h) from model-based samples was used to calculate the ratio of fermentation with iron reduction divided by fermentation without iron reduction for the reactions of glycolysis, fermentation, citric acid cycle and the pentose phosphate pathway. Grey lines show reactions where no flux was present in the model and gaps in the values within the figure legend indicate that these range was not represented. Flux ranges greater than 1 show the reactions with higher flux ranges in fermentation with iron reduction and those less than 1 show those with higher flux ranges in fermentation without iron reduction.

Fig. S7. Minimal reaction subnetwork (MRS) for fermentation with and without iron reduction with reduced

ferredoxin as electron donor. The minimum reaction set that is necessary to allow the transformation of the substrate into experimentally observed products. Black arrows show reactions present in all or some MRS (necessary); green arrows show reactions present in some MRS of fermentation with iron and present in all MRS of fermentation alone; and red arrows show reactions present in some MRS of fermentation with iron, but not present in any MRS of fermentation alone. Grey arrows are reactions not present in the MRS.

Fig. S8. Comparison of growth measurement methods. (A) protein (squares) and CFU mL⁻¹ (triangles) or (B) OD₆₀₀ (circles) and CFU mL⁻¹ (triangles). *C. acetobutylicum* was grown in fermentation with 0.5% glucose.

Table S1. Carbon and electron balance at 24 h of *C. acetobutylicum* with and without iron reduction. The oxidation–reduction balance was calculated by dividing the sum of the number of electrons gained by the products relative to glucose by the sum of the number of electrons lost by the oxidized products relative to glucose: (mmol acetate*0 + mmol butyrate*4 + mmol ethanol*4 + mmol acetone*4 + mmol butanol*8 + mmol H₂*2 + mmol Fe²⁺*1) divided by (mmol pyruvate*2 + mmol CO₂*4 + mmol TIC*4). In addition, ATP was measured.

Table S2. List of reactions in which non-overlapping flux ranges were observed for fermentation with and without Fe(III)-citrate (at the 6-h time point).